journal

J. Am. Ceram. Soc., **93** [6] 1650–1662 (2010)
DOI: 10.1111/j.1551-2916.2010.03613.x

The Predictive Power of Electronic Polarizability for Tailoring the Refractivity of High-Index Glasses: Optical Basicity Versus the Single Oscillator Model

John McCloy,*,† Brian Riley,* Bradley Johnson,* Michael Schweiger, and Hong Amy Qiao

Pacific Northwest National Laboratory, Richland, Washington 99352

Nathan Carlie*

Clemson University, Clemson, South Carolina 29634

High-density (~8 g/cm^3) heavy metal oxide glasses composed of PbO, Bi_2O_3, and Ga_2O_3 were produced, and refractivity parameters (refractive index and density) were computed and measured. Refractive indices were measured at six discrete wavelengths from 0.633 to 10.59 μm using a prism coupler, and data were fitted to the Sellmeier expression. Optical basicity was computed using three models—average electronegativity, ionic-covalent parameter, and energy gap—and the results were used to compute oxygen polarizability and subsequently the refractive index. Single oscillator energy and dispersion energy were calculated from experimental indices and from oxide energy parameters. The predicted glass index dispersion based on oxide oscillator parameters underestimates the measured index by only 3%–4%. The predicted glass index from optical basicity, based on oxide energy gaps, underpredicts the index at 0.633 μm by only 2%. The calculated glass energy gap based on this optical basicity overpredicts the experimental optical gap by 6%–10%. Thus, we have shown that the density, the refractive index in the visible, and the energy gap can be reasonably predicted using only composition, optical basicity values for the constituent oxides, and partial molar volume coefficients. The relative contributions of the oxides to the total polarizability were assessed, providing an additional insight into controlling the refractivity of high-index glasses.

I. Introduction

The refractive index as a function of wavelength is a critical design parameter for advanced photonic systems. Thus, the ability to estimate the refractivity of glasses based solely on their composition is of great value to both photonic designers and the materials scientists supporting those designs. Lead–bismuth–gallate glasses were reported by Corning in the early 1980s, and their large electro-optic and magneto-optic constants, infrared transmittance, and large index of refraction were identified.[1,2] Since then, there has been further interest in these materials for use in nonlinear optics, specifically a second harmonic generation, due to their large nonlinear refractive index.[3,4] Glasses produced with ≥50 cation% of Bi and/or Pb are called heavy metal oxide glasses.[5]

One concept often seen in the literature to explain the refractive index of oxides is polarizability (or alternately, the ionic refractivity), both of the cations and of oxygen. Usually, the refractive index is known or measured, and then the polarizability is calculated, such as with the Lorentz–Lorenz equation (see Eq. (5) below). In this study, the process was approached from the opposite direction, that is, the refractive index was predicted on the basis of polarizability determined some other way. In this case, we chose to use correlations of polarizability with optical basicity, along with various tabulated scales of optical basicity (based on average electronegativity [EN], ionic-covalent parameter [ICP], or energy gap), to predict the refractive index. Creating a density model facilitated the prediction of the other parameter necessary to calculate the index through the Lorentz–Lorenz equation.

Measurements of density and refractive index were made in parallel. Index data were collected through the entire infrared atmospheric window (i.e., 0.6328–10.591 μm). To our knowledge, the wavelength dependence of polarizability has been investigated in the infrared only by Zhao *et al.*,[6] who looked at bismuth–borate glasses up to 1.5 μm. The current study, therefore, further refines the understanding of oxygen polarizability in heavy metal oxide glasses out to mid- and long-wave infrared (i.e., 3–12 μm).

This paper first describes in some detail the theoretical background and three different methods for determining optical basicity based on optical properties and chemical bonding. Specifically, the results from UV absorption, refraction in glasses and oxides, and the energy gap were used as the "optical properties" method for determining optical basicity. This is in contrast to the other two methods, which are based on chemical bonding considerations, including atomic and ionic radii, valence, and EN. The rest of the paper addresses a density model, a refractive index prediction, and a band gap prediction, in comparison with their respective experimental measurements for this particular lead–bismuth–gallate system.

II. Optical Basicity

Optical basicity is fundamentally related to the chemical bonding in a solid and is related to the optical properties of a material through the polarizability of electron clouds around atoms (ions) by electromagnetic waves. Optical basicity can be seen as describing the Lewis acid–base relationship where the acidic probe ion allows the electronic charge donation power of the anion (usually oxygen) to be determined.[7] Optical basicity should be considered a material property of a system in the same way that iconicity and EN is because it too is closely related to chemical bonding. Like these other chemical parameters, there are many ways to measure or calculate optical basicity, but in some cases, the resulting scales are mutually exclusive. This can lead to misapplications of the derived empirical correlations to optical basicity in the literature if the wrong basicity scale is used. The following treatment is an effort to clarify the theoretical background for the optical basicity scales based on "optical properties" (UV absorption, refractivity, and energy gap), average EN, and the somewhat hybrid approach based on the ICP.

W. Mullins—contributing editor

Manuscript No. 26513. Received July 9, 2009; approved December 15, 2009.
Pacific Northwest National Laboratory (PNNL) is operated for the U.S. Department of Energy by Battelle under Contract DE-AC05-76RL01830.
*Member, The American Ceramic Society.
†Author to whom correspondence should be addressed. e-mail: john.mccloy@pnl.gov

The concept of optical basicity has gained wide acceptance and utility since its introduction in the early 1970s by Duffy and Ingram.[8] Optical basicity concepts have been applied to understand and predict the refractivity of glasses,[9,10] nonlinear optical properties,[11] the reduction–oxidation of cations,[12–14] the behavior of extractive metallurgical slags,[15–18] and even the behavior of catalysts.[19] Optical basicity has been shown to be closely related to parameters describing the chemical bonding in oxides, including electronic polarizability of oxygen, EN (variously conceived),[20,21] the Racah parameters,[12,14,22] the energy gap,[20] and the oxygen-binding energy.[23]

(1) Optical Basicity and Optical Properties

Optical basicity, as originally conceived, measured the electron donation power of oxygen to a specific probe ion. Oxides were doped with a $d^{10}s^2$ probe ion (Tl^+, Pb^{2+}, or Bi^{3+}) that absorbs in the ultraviolet (UV) and whose peak absorption due to the $^1S_0 \rightarrow {}^3P_1$ electronic transition allowed by spin–orbit coupling undergoes a wavelength shift, depending on the local electronic environment. Procedurally, optical basicity was a measure of how much the primary UV absorption wavenumber of the probe ion shifted in a pure or a mixed oxide (ν_{glass}) in comparison with its spectral position as a free ion (ν_{free}) and in CaO (ν_{CaO}, as a standard), which can also be thought of as the ratio of Jørgensen's nephelauxetic h parameter[24] in the medium and in CaO.

$$\Lambda_{glass} = \frac{\text{Electron donor power of glass/slag}}{\text{Electron donor power of CaO}} = \frac{\nu_{free} - \nu_{glass}}{\nu_{free} - \nu_{CaO}} = \frac{h(\text{medium})}{h(\text{CaO})} \quad (1)$$

where Λ_{glass} is the optical basicity. This procedure allowed determination of the optical basicity for a number of alkali and alkaline earth oxides as well as some of the primary glass-forming oxides, including Si, B, and Al. Optical basicity was found to be additive in mixed oxide glasses according to

$$\Lambda_{glass} = \sum_i X_i \Lambda_i \quad (2)$$

where X_i is equivalent fraction of the cations for the i-th $AO_{a/2}$ oxide, and Λ_i is the optical basicity of the i-th component oxide. Here the oxides have been normalized to single cations, where for an oxide A_pO_q consisting of A^{a+} cations, $\Lambda(AO_{a/2}) = 1/\gamma_A$ and $a = 2q/p$. This calculation of optical basicity of a glass from the component oxides with tabulated basicities is often called the "theoretical basicity" (Λ_{th}).

Another way this expression can be conceived is through the idea of a basicity-moderating parameter γ, which is specific to a cation and represents the polarizing power of the cation.

$$\Lambda = \sum_i \frac{z_i r_i}{2} \frac{1}{\gamma_i} \quad (3)$$

where z_i is the cation valence or oxidation number and r_i is the ionic ratio with respect to the number of oxygens (i.e. the number of each cation available divided by the total number of oxygens in the system). For a single oxide, the basicity moderating parameter is simply the inverse of the optical basicity. Perhaps more simply, it can also be seen that the following relation is fully equivalent to the above relations, where q_i is the number of oxygen atoms in the oxide and x_i is the mole fraction of the i-th component oxide[25]:

$$\Lambda_{glass} = \sum_i x_i q_i \Lambda_i / \sum_i x_i q_i \quad (4)$$

The lack of UV transparency of transition metal oxides led to consideration of another method for determining optical basicity using refractivity (refractive index and density).[26,27] Subsequently, Duffy and others determined the optical basicities of oxides by investigating refractivity data (refractive index and density) for various binary oxides and oxide glasses.

Empirical relations have been found between the oxygen polarizability (α_{ox}) as calculated by the Lorenz–Lorentz equation and optical basicity. The Lorenz–Lorentz equation allows the molar polarizability (α_m) of the solid to be calculated on the basis of Avogadro's number (Nav), its molecular weight or formula weight (M), density (ρ), and refractive index (n, at infinite wavelength but normally taken as the sodium D line). The polarizability per oxygen (α_{ox}) is determined by subtracting the cation electronic polarizabilties ($\alpha_{cat,i}$) (as tabularized or calculated from cation refractivity [R_i][28–33]) and then dividing by the total number of oxygens in the formula unit. Polarizability is typically expressed in units of $Å^3$, and calculations are performed in the Gaussian (cm–g–s or cgs) units system because it is more convenient.

$$\alpha_m(Å^3) = \frac{3}{4\pi}\frac{M}{\rho N_{AV}}\left(\frac{n^2-1}{n^2+2}\right)\left(10^{24}\frac{Å^3}{cm^3}\right) = 0.397\left(\frac{Å^3\,mol}{cm^3}\right)\frac{M}{\rho}\left(\frac{n^2-1}{n^2+2}\right) \quad (5)$$

In the glass literature, it is often more common to see the mention of ionic refractivity (R_i) rather than electronic polarizability of the ion (α_i), which is simply related as:

$$R_i\left(\frac{cm^3}{mol}\right) = \frac{4\pi}{3}N_{Av}\alpha_i(cm^3) = 2.52\left(\frac{cm^3}{Å^3\,mol}\right)\alpha_i(Å^3) \quad (6)$$

An empirical relation between the optical basicity of a given oxide system and the electronic polarizability of oxygen based on refractivity data for binary oxides has been found[34]:

$$\Lambda = 1.67\left(1 - \frac{1}{\alpha_{ox}}\right) \quad (7)$$

and more recently, a different empirical relation was published based on a series of oxide glasses.[35]

$$\Lambda = \frac{(3.133\alpha_{ox} - 2.868)^{1/2}}{1.567} - 0.362 \quad (8)$$

The optical basicity of a glass is assumed to represent the average oxygen environment throughout the material. It is clear, however, that the charge on the oxygen atoms can be very different locally such as occurs with nonbridging oxygen.[36] Duffy and Ingram[9] noted this from the beginning and referred to it as the microscopic optical basicity, observed when using different probe ions on a single material. Later, it was determined that the local coordination number (CN) and the ligand configuration of the cations play a key role as well, resulting in multiple values for optical basicity for boron,[35] aluminum,[37] germanium,[38] and phosphorus determined by refractivity.[18,39] The optical basicity of glasses as determined by probe ion spectroscopy (Λ_p) often differed slightly from the more complete but more variable set of basicities determined from refractivity (Λ_n).[35]

In addition to determinations of basicity from refractivity data, correlations have been shown between the energy gap (E_g) in oxides and refractivity as[20]

$$E_g = 20\,(1 - R_m/V_m)^2 \text{ or } (E_g)^{1/2} = 4.47(1 - R_m/V_m) \quad (9)$$

where R_m is the molar refractivity in cm^3/mol as determined from the molar polarizability (α_m) as shown in (6) and V_m is the molar volume in cm^3/mol.

$$V_m = \sum x_i M_i / \rho_{glass} \quad (10)$$

The parameter R_m/V_m term characterizes the insulator to metallic behavior transition, which results in metallic behavior when it approaches unity. Dimitrov and Sakka[40] have calculated and compared the optical basicity of various oxides using oxygen polarizability determined from refractivity. They also used band-gap data and found a reasonable agreement for most oxides. A slightly different form for the relation of the energy gap to refractivity has been proposed to include data from glass systems with highly polarizable cations (e.g., Pb, Cd, Ti, and Te), including heavy metal oxides, phosphates, fluorides, and chalcogenides[41,42]:

$$(E_g)^{1/2} = 1.23(1 - R_m/V_m) + 0.98 \quad (11)$$

In our work, we found that this latter equation represented the data for heavy metal oxides much better than the original relation as suggested by Duffy (Eq. (9)).

(2) Optical Basicity and EN

Given the importance of EN as related to optical basicity, it is instructive to review a brief history of the theoretical developments leading to the optical-basicity scales derived from average EN and the ICP used here.

Early on, it was pointed out that there existed some empirical correlations between the optical basicity of oxides and EN as variously conceived. Pauling (1932)[43] thought of EN as the power of the atom in a molecule to attract electrons to itself, and derived his scale from thermochemical heats of formation on an arbitrary scale from 4 (fluorine) to 0.7 (cesium). He did not account for the valence state or the ionic radius but had a single value for each element. This value was conceived of as an assessment of the ionic contribution to essentially covalent bonding. The Pauling EN for the cation ($\chi_{M,Paul}$) can be correlated to optical basicity, but only to a cation whose oxidation state corresponds to a noble gas electron configuration.[44–46] A number of additional EN scales have been proposed over the years since Pauling's first introduction of the idea.[47,48] Fundamentally, bonding in compounds exhibits a mixed nature of electrovalent (ionic) and covalent forces. Many of the theories of EN have sought to account for both these forces in bonding. Even though EN in principle is a property of elements, the units for EN differ considerably, depending on the derivation.[49]

The concept of "average EN" was introduced by Asokamani and Manjula[50] to help understand the behavior of oxide superconductors. Average EN, or χ_{ave}, is expressed as

$$\chi_{ave} = \sum_{i=1}^{n} \chi_i N_i / \sum_{i=1}^{n} N_i \quad (12)$$

where N_i is the number of atoms of a particular element and χ_i is the element's Pauling EN. This relation has been used by Reddy *et al.*[51] to convert the relationships derived by Duffy for optical basicity and the Pauling EN into a relationship between optical basicity and average EN. The following relationship is derived between average EN and optical basicity for simple binary oxides[21]:

$$\Lambda = 1.59 - 0.2279\chi_{ave} \quad (13)$$

Recently, Zhao *et al.*[52] modified the use of the average EN for the lanthanides, this time carrying out the calculations based on EN values different from those of Pauling, but otherwise the same calculation as Eq. (12). These researchers chose for their scale the EN as determined by Li and Xue.[47] Li and Xue's EN (Eq. (14)) is very similar in form to the earlier Zhang[53] EN (Eq. (15)). However, the former uses the inverse of Shannon's "crystal radii" for six coordinated ions (r_{cr}) rather than the inverse of the covalent radius (r_{cov}^2) squared as Zhang did. By plotting the Pauling EN versus the effective ion potential (Z^*/r_{cr}, Li & Xue) or versus the electrostatic force (Z^*/r_{cov}^2, Zhang), one obtains the EN:

$$\chi_{Li} = 0.105\frac{Z^*}{r_{cr}} + 0.863 = 0.105\frac{n^*(I_z/R_\infty)^{1/2}}{r_{cr}} + 0.863 \quad (14)$$

$$\chi_Z = 0.241\frac{Z^*}{r_{cov}^2} + 0.775 = 0.241\frac{n^*(I_z/R_\infty)^{1/2}}{r_{cov}^2} + 0.775 \quad (15)$$

Here χ_{Li} is the EN as a function of the effective nuclear charge on the valence electrons (Z^*), which is itself a function of the effective principal quantum number (n^*), the ultimate ionization potential (I_z), and the Rydberg constant ($R_\infty = 13.6$ eV).

Concepts that include both ionic and covalent contributions to bonding have also been tied to notions of optical basicity. Portier *et al.*[54] proposed the concept of an ICP (Eq. (16)), similar to Zhang's earlier concept of acid strength[55] ($\boldsymbol{Z}$, Eq. (17)), to account for the variations due to a differing CN and hence the ionic radius.

$$ICP = \log P - A\chi + B = \log(z/r_i^2) - A\chi + B \quad (16)$$

$$Z = P - 7.7\chi_Z + 8.0 = z/r_i^2 - 7.7\chi_Z + 8.0 \quad (17)$$

Here P is the polarizing power of the ion, formulated as the atomic charge z divided by the ionic radius r_i, A and B are fit coefficients depending on the choice of EN scales and radii scales (i.e., Shannon's "ionic radii" or "crystal radii"),[56] and the ICP of Au^+ is set equal to zero as the standard. Thus, the calculated ICP is dependent on the assumed inputs, and so caution should be exercised with tabularized data. The ICP was shown to correlate well with bond stability, formation enthalpy, and fusion temperature.

Furthermore, Portier *et al.*[48] plotted Zhang's EN (χ_z) divided by the ionic radius against the oxidation state divided by the atomic radius, using $r_{ox} = 1.40$ Å (Shannon's "ionic radius"). By linear regression, they determined EN (χ_{Port}), which is only a function of cation charge (z) and ionic radius (r_i). A small elemental-specific correction term (α, tabulated by Portier *et al.*[48]) was added back to align the data to Zhang's EN. The final EN relation is

$$\chi_{Port} = 0.274z - 0.15zr_i - 0.01r_i + 1 + \alpha \quad (18)$$

Then, using this definition of EN (χ_{Port}) and Shannon's "ionic radii" and assuming that six coordinated Au^+ have zero ICP, the ICP is determined from Eq. (16) to give

$$ICP_{(Port)} = \log P - 1.38\chi_{Port} + 2.07 = \log(z/r_i^2) - 1.38\chi_{Port} + 2.07 \quad (19)$$

Finally, Lebouttier and Courtine used this last value of $ICP_{(Port)}$ and correlated it to optical basicity.[57] The ICP was determined for various ions in specific coordinations (e.g., tetrahedral, octahedral). The optical basicity of the cation in

this coordination was determined from existing optical basicity data (determined by other means) for oxides and glasses. From here, Lebouttier and Courtine divided the ions into groups of the same valence electronic configuration: *sp*, $d^{10}s^2$, d^0, d^{10}, and d^1–d^9. The first group of *sp* ions (e.g., alkali [+], alkaline earth [2+], B^{3+}, Al^{3+}, Si^{4+}, and P^{5+}) had been those originally investigated by Duffy's probe ion technique because they allowed viewing the UV absorption shift of the probe ion. For other groups, other methods for determining optical basicity were required, such as review of refractivity data. Essentially, these authors drew linear fits in each electronic configuration group between the ICP and the known optical basicity. From there, they postulated that these relations could be extrapolated to ions in coordinations, spin states, and valence states where optical basicity was not known. Hence, they provided a method for predicting the optical basicity (hereafter referred to as Λ_{ICP}). The linear relations found were of the form (only two of five relations are shown, those relevant to the heavy metal oxides studied here):

$$\begin{aligned} d^{10}s^2 &: \mathrm{ICP} = -13.844\Lambda + 17.134 \\ d^{10} &: \mathrm{ICP} = -0.729\Lambda + 1.390 \end{aligned} \tag{20}$$

Optical basicity derived from ICP then represents a hybrid scale because the equations are anchored to *measured* basicity values from optical properties, but unknown configurations (coordinations, valence, and spin states) are calculated from the ICP, which is only dependent on valence and ionic radius. The authors apply these relations to predict the basicity of many mixed oxides for which it is desirable to understand the acid–base properties for application to solid-state catalysis. The relationship between the Racah parameter and the optical basicity and ICP has also been investigated in relation to the inductive effect (polarization of one bond due to polarization of adjacent ones) and magnetic ordering in solids.[22]

Now that the theoretical basis for the optical basicity scales based on optical properties, average EN, and ICP has been reviewed, it will be shown that, of the three, the scale based on optical properties is the most reliable for predicting the refractive index and energy gap. Furthermore, these predictions based on optical basicity are superior to others based on single oscillator parameters.

III. Experimental Procedure

(1) Density—Prediction and Measurement

Four different lead bismuth gallate glasses were prepared for this study with varying quantities of high-purity PbO (Fisher Scientific; Pittsburgh, PA), Ga_2O_3 (Alfa Aesar; Ward Hill, MA), and Bi_2O_3 (Alfa Aesar); the glass compositions are listed in Table I. The glasses were mixed in an agate mill for 5 min, heated in Pt/10% Rh crucibles at 900°–950°C for 20–30 min, and poured on a steel quench plate to prevent crystallization. Estimated viscosities of these glasses were on the order of 0.1 Pa·s at these processing temperatures.

Table I. HMO Glass Compositions (in mol%), Densities (in g/cm^3)

Glass compositions	Ga_2O_3	PbO	Bi_2O_3	ρ (Arch)	ρ (Pycn)	ρ (Calc)	M (g/mol)
HMO-1	23.0	47.5	29.5	8.028	8.138	8.041	286.59
HMO-2	15.0	37.0	48.0	8.358	8.422	8.444	334.36
HMO-3	15.0	42.5	42.5	8.361	8.368	8.409	321.01
HMO-4	20.0	40.0	40.0	8.206	8.172	8.230	313.15

Table II. Molecular Weight (M) and Partial Molar Volume (v_i) Coefficients Obtained Using Least Squares Method

Component	M_i	v_i
Bi_2O_3	466.0	51.503
Ga_2O_3	187.4	36.020
PbO	223.2	25.608

Measured densities of the glasses were obtained using two methods: helium pycnometry and the Archimedes method using deionized water (DIW). Helium pycnometry was performed using a Micromeritics (Micromeritics Instrument Corporation, Norcross, GA) Accupyc 1330 pycnometer with ultra-high purity helium as the filler gas. The Archimedes method was performed using the MCC-12 test method and a Sartorius A200S analytical balance (Sartorius, Goettingen, Germany).

To develop a predictive density model for lead bismuth gallate glasses, SciGlass® 7.0[58] (Build 7.10.05.098, ITC Inc., Hamilton, OH) was used to compile the literature data for all glasses composed exclusively of Bi_2O_3, PbO, and Ga_2O_3 with ≥ 50 cation% of Bi+Pb (in the form of Bi_2O_3 and PbO), and that included measured density values.[1,5,59–78] Of the 24 studies that produced glasses fitting these criteria, all data from 22 of the studies in addition to the eight measured data points mentioned above (four glasses measured using both DIW Archimedes and He pycnometry methods) were kept for model development, yielding 59 total data points. The two studies that were excluded from the model showed erratic data.[79,80] Using the remaining 59 data points, a least-squares method was implemented to calculate partial molar volumes, v_i, for the three glass constituents, and these values are presented in Table II. Once v_i values were obtained, densities were calculated for all of the glasses used to create the model, including the four glasses prepared for this study as follows:

$$\rho_{\mathrm{calc}} = \frac{M}{V_{\mathrm{m}}} = \frac{\sum_{i=1}^{n} x_i M_i}{\sum_{i=1}^{n} x_i v_i} \tag{21}$$

where M is the total molecular weight (g/mol) of the glass, V_{m} is the molar volume of the glass (cm^3/mol), x_i is the i-th component mole fraction, M_i is the i-th component molecular weight, and v_i is the i-th component partial molar volume and ρ_{calc} is in g/cm^3.

The measured densities and calculated densities are shown in Table I and Fig. 1. Measured densities were within ±1% of the values predicted from partial molar volume calculations.

(2) Refractive Index—Prediction

Optical basicities of the component oxides as determined from the various methods described earlier are shown in Table III. Because of having complete datasets, optical basicities determined from (1) average EN ($\Lambda_{\chi av}$), (2) ICP (Λ_{ICP}), and (3) oxide band gaps Λ_{E_g} were used to calculate optical basicities of the glasses.

Table IV shows the computed optical basicities of these glasses used to determine the total molar polarizability through Eq. (5). The use of Eq. (8), derived originally from glass refractivity data, gave consistently lower predicted polarizability and hence index than Eq. (7), which was derived originally from probe ion data. Equation (7) is the preferred one used in the literature and gave index predictions closer to the measured values.

For an oxide A_pO_q, the total molar polarizability (α_m), being the sum of the molar cation polarizability ($\alpha_{m,cat}$) and the molar oxygen polarizability ($\alpha_{m,ox}$), was used in the Lorentz–Lorenz

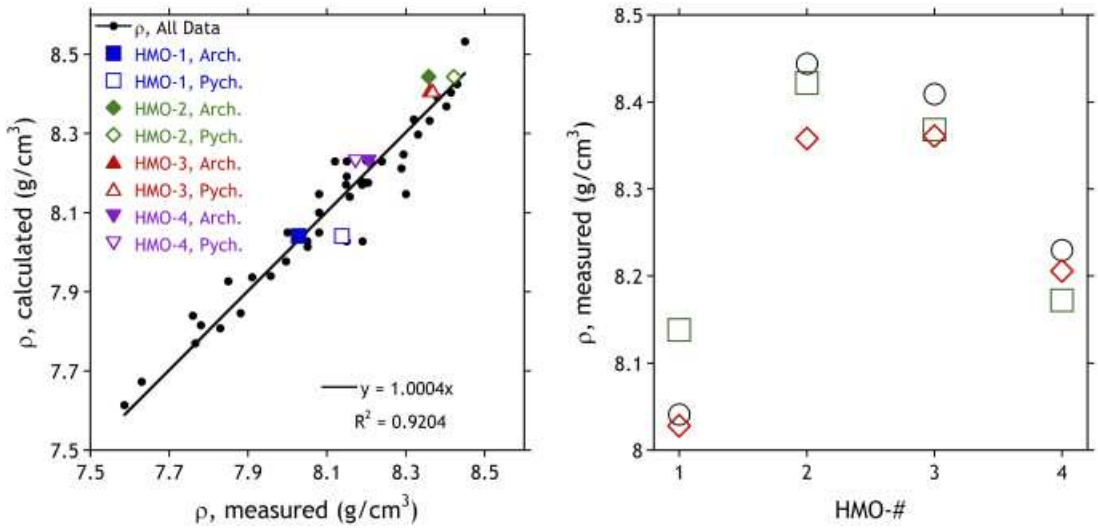

Fig 1. (A, L) Calculated versus measured densities for lead–bismuth–gallate glasses used to develop the density model. HMO-1, -2, -3, and -4 glasses are included in the plot. (B, R) Calculated (circles) versus measured (squares—pychnometry, diamonds—Archimedes) densities for only HMO glasses; agreement is within ±1%. Error of 0.005% associated with Archimedes measurements according to calibration with copper standard results in error bars smaller than the symbols. Such a standard was not available for the pycnometer.

Eq. (5), along with the density determined from the Archimedes measurement, to determine the refractive index.

$$\alpha_m = \sum_i x_i q_{ox}, i^{\alpha}_{ox,i} + x_i p_{cat,i} \alpha_{cat,i} = F_{ox}\alpha_{ox} + \alpha_{m,cat} = \alpha_{m,ox} + \alpha_{m,cat} \quad (22)$$

The polarizability per oxygen (α_{ox}) is determined from the total molar polarizability by subtracting the molar cation polarizability ($\alpha_{m,cat}$) and dividing by the fractional oxygens (F_{ox}, i.e., mole fraction oxide $x_i^* q_{ox,i}$, oxygens per oxide). The cation term and fractional oxygen term do not change for a given composition. Only the predicted total molar polarizability changes, depending on assumed optical basicity, and the differences are reflected in the polarizability per oxygen listed in Table IV for each method. For the EN method, gallium was assumed to be 4-coordinated, bismuth 6-coordinated, and lead 4-coordinated (see "Section IV"). The predicted refractive indices track with the calculated optical basicities as follows:

$$n_{Eg} > n_{ICP} > n_{\chi av} \text{ since } \Lambda_{Eg} > \Lambda_{ICP} > \Lambda_{\chi av}$$

3 *Refractive Index—Measurement*

The refractive index was measured at five discrete wavelengths using a modified prism coupler setup (Metricon 2010, Pennington, NJ). Laser wavelengths included 0.6328 μm (HeNe), 1.5473 μm (Er-doped telecom), 3.391 μm (HeNe), 5.348 μm (quantum cascade laser), 9.536 μm (CO_2), and 10.591 μm (CO_2). Prisms used were rutile (0.6328 and 1.5473 μm) or gallium phosphide (all wavelengths). A germanium detector was used for 0.6328 and 1.5473 μm, and a Hg–Cd–Zn–Te detector was used for 3.391, 5.348, 9.294, and 10.591 μm. The precision in the measurement of bulk samples is 5×10^{-4}, provided that the prism index is known as a function of temperature, and the knee in the curve due to the onset of total internal reflection is resolvable. In some cases, particularly at the longer wavelengths, fringing was observed, and the knee was difficult to resolve, leading to degraded precision. Table V shows the measured index data for the glass compositions at six wavelengths in the visible and infrared as well as the assumed indices of the prisms at the wavelengths used. Measurements were all taken at room temperature, with ambient laboratory temperatures known to fluctuate within 25° ± 4°C.

Six-parameter Sellmeier equations were fitted to these datasets, and the parameters are shown in Table VI.

Table III. Optical Basicity of Oxides in HMO Glasses as Determined by Various Means

Symbol	Λ_n	$\Lambda_{\chi_{av}}$	Λ_{ICP}	Λ_n	Λ_{E_g}	α_{cat}	A_{int}
Input data→	Glass refractivity data (Eq. (7))	Tabulated L&X[47] EN(Eq. (13))	ICP correlations in L&C[57](Eq. (20))	Refractive index of oxide (Eq. (7))	Band gap of oxide[40](Eq. (9))	Cation polarizability (Å^3)[40]	Interaction parameter (Å^{-3})[23]
Ga_2O_3 (d^{10})	0.71[81]	0.92 (CN = 4) 0.93 (CN = 6)	0.52 (CN = 4) 0.72 (CN = 6)	0.71[40]	0.80	0.195	0.126
PbO ($d^{10}s^2$)	0.96[82]	1.01 (CN = 4) 1.02 (CN = 6)	1.19 (CN = 4) 1.19 (CN = 6)	1.19,[40] 0.95[83]	1.17	3.623	0.005
Bi_2O_3 ($d^{10}s^2$)		0.945 (CN = 5) 0.949 (CN = 6)	1.184 (CN = 5) 1.185 (CN = 6)		1.19	1.508	0.008
Bi_2O_5 (d^{10})		0.855 (CN = 6)	1.08 (CN = 6)				

For Ga^{3+}, CN = 6 corresponds to the oxide, CN = 4 to the glass.[84] For Bi^{3+}, both CN = 5 and CN = 6 are seen in glasses as in the oxide[85]; data for Bi^{5+} are included for reference only. For Pb^{2+}, CN = 4 seen in PbO and glasses; CN = 3 in glasses[85]; no radius data available in Shannon or EN data available in Li and Xue for CN = 3; data for CN = 6 included for reference only. Cation polarizabilities calculated from ionic refractivity data as $\alpha = R/2.52$.

Table IV. Computed Optical Basicities and Refractive Index via Three Methods

Glass compositions	A_{int} (Å^{-3})	$\alpha_{m,cat}$ (Å^3)	F_{ox}	$\Lambda_{\chi_{av}}$	α_{ox} (χ_{av})	n (χ_{av})	Λ_{ICP}	α_{ox} (ICP)	n (ICP)	Λ_{E_g}	α_{ox} (E_g)	n (E_g)
HMO-1	3.37	2.70	2.05	0.953	2.33	2.088	0.96	2.36	2.102	1.05	2.71	2.281
HMO-2	2.46	2.85	2.26	0.953	2.33	2.035	1.05	2.71	2.214	1.11	2.98	2.360
HMO-3	2.44	2.88	2.15	0.955	2.34	2.059	1.05	2.68	2.223	1.10	2.95	2.371
HMO-4	3.04	2.73	2.20	0.952	2.33	2.058	1.00	2.51	2.145	1.08	2.83	2.315

$$n^2(\lambda) = 1 + \frac{A\lambda^2}{\lambda^2 - B^2} + \frac{C\lambda^2}{\lambda^2 - D^2} + \frac{E\lambda^2}{\lambda^2 - F^2} \tag{23}$$

Figure 2 shows the measured and computed refractive index dispersion for the glasses.

Comparison of the smallest wavelength measured datapoint (0.6328 μm) with the predictions for the refractive index based on optical basicity in Table IV shows that calculating from the optical basicity parameters from the band gap of the oxides, n_{E_g}, yields the best correlation with the measured values.

Figure 3 shows the per oxygen polarizability dispersion computed from Eq. (5) using the measured refractive index.

(3) Optical Gap and Dispersion

Transmission of the glasses was measured from 0.2 to 3.3 μm at 0.1 s/nm dwell and 1 nm intervals using a Varian Cary 500 dispersive spectrophotometer (Varian Inc., Palo Alto, CA) and from 2.5 to 25 μm using 128 coadded scans at 2 cm^{-1} resolution using a Thermo Nicolet 6700 Fourier transform infrared spectrometer (Thermo Fisher Scientific, Waltham, MA). The absorption coefficient was calculated from the Beer–Lambert law assuming no reflections in the high absorption band edge as:

$$\beta = -(1/L)\ln(T) \tag{24}$$

and alternately assuming multiple reflections as:

$$\beta_{mr} = (1/L) \times \ln\left[(1-R)^2/2T + \sqrt{R^2 + (1-R)^4/4T^2}\right] \tag{25}$$

where β is the absorption coefficient (in cm^{-1}), L is the sample thickness, T is the measured transmittance, and R is the single surface reflectivity in air calculated from the index of refraction. Reflection is calculated from the Sellmeier refractive index as

$$R = (n-1)^2/(n+1)^2 \tag{26}$$

From these calculated absorption coefficients, the Tauc plot and the Urbach plot were generated.

Optical energy gap (E_{opt}) was determined using Tauc's method[86] of extrapolating $(\beta h\nu)^{1/2}$ [eV$^{1/2}$/cm$^{1/2}$] vs energy [eV] to zero using the equation:

$$\beta(\nu) = \text{constant}\left[(h\nu - E_{opt})^2/h\nu\right] \tag{27}$$

where ν is the frequency and h is Planck's constant. Strictly speaking, Tauc's law should only be applied to calculated absorption coefficients above 10^4 cm^{-1}, whereas, given the thickness of our samples (~2 mm), the calculated absorption coefficients at the edge of transmission are about 5×10^2 cm^{-1}. However, this region is still very linear as shown in Fig. 4. Urbach energy (ΔE_{Urb}) was determined from the slope of the linear part of the plot of ln β versus energy.[87]

$$\ln\beta(\nu) = [h\nu/\Delta E_{Urb}] - \text{constant} \tag{28}$$

The exponential increase of absorption near the absorption edge is a result of transitions between the density-of-states tails caused by disordering. For noncrystalline solids, the broadened absorption edge compared with crystals arises not only from electric fields due to longitudinal optical phonons and charged impurities as for crystals but also from density fluctuations, charged defects, and lack of long-range ordering.[88] The Urbach energy is the absorption edge energy width of the localized states, and absorption is from these states to the extended valence band. Increases in Urbach energy are interpreted as increased local disorder.[89] Urbach energy is the lowest for HMO-2 and HMO-3, and these glasses have the highest Bi_2O_3 content. Additions of Bi_2O_3 have been shown by an extended X-ray absorption fine structure (EXAFS) to reduce the quantity of nonbridging oxygens in Ga_2O_3–PbO–Bi_2O_3 glasses, as Bi can maintain coordinations of five or six oxygens.[85] It is possible that the decrease of the Urbach energy is due to the reduction in the electrical fields around nonbridging oxygens.

Equations (9) and (11) show how the energy gap of the glasses should be related to the ratio of the molar refractivity to the molar volume (R_m/V_m). For this assessment, the refractivity was determined from Eq. (6), using the total molar polarizability determined from the optical basicity of oxide band gaps, and the molar polarizability was determined from the Archimedes density and glass compositions. The results of the experimentally determined energies and calculated R_m/V_m ratios are shown in Table VII. The values for E_{opt} and ΔE_{Urb} in this table are calculated from the absorption as determined from Eq. (25), whereas using Eq. (24) resulted in slightly higher absorptions and thus lower estimates of E_{opt} by about 0.02 eV. Changes to the Urbach energy were much larger, about a factor of two

Table V. Measured Refractive Indices of Glasses

Glass Compositions	0.6328 μm	1.5473 μm	3.391 μm	5.348 μm	9.294 μm	10.591 μm
HMO-1	2.3153*	2.2184*	2.1879	2.1509	Not tested	1.9447
HMO-2	2.4008	2.2870	2.2595	2.2181	2.0772	2.0035
HMO-3	2.3882	2.2750	2.2475	2.2082	2.0621	1.9897
HMO-4	2.3551	2.2492	2.2221	2.1796	2.0275	1.9652
GaP prism	3.3079	3.0558	3.0238	3.0085	2.9744	2.9571
*Rutile prism	2.8647	2.6049				

*after index value indicates it was determined using the rutile prism. All others used the GaP prism. Precision is ±0.001 due to uncertainty in the temperature, but the method is capable of an order of magnitude better with precise temperature control, so the final significant digit is retained.

Table VI. Sellmeier Parameters

Glass Compositions	*A*	*B*	*C*	*D*	*E*	*F*
HMO-1	1.3556	6.937E–07	2.5151	0.2562	7.2321	29.260
HMO-2	1.5014	0.33549	2.6789	−5.4960E–07	5.6872	25.621
HMO-3	1.4813	0.33539	2.6470	1.9808E–07	5.3683	24.956
HMO-4	1.4253	0.33004	2.5929	−1.8371E–07	9.2680	31.557

larger when using Eq. (25) as opposed to Eq. (24). Comparison of the predictions for energy gap from Eqs. (9) and (11) with the experimentally derived optical gap shows that the more recently determined Eq. (11) is a much better prediction of the optical gap (about a 10% overestimate) than is Eq. (9) (about a 50% overestimate).

Wemple and DiDomenico[90] have described how to model refractive index (n) data in a single oscillator model as a function of energy (E) as:

$$n^2 - 1 = \frac{E_0 E_d}{E_0^2 - E^2} - \frac{E_l^2}{E^2} \tag{29}$$

using three parameters: E_0 the single oscillator energy, E_d the dispersion energy describing the strength of interband transitions, and E_l the lattice contribution to near band edge absorption,[91] all values in eV. In amorphous solids, E_d has been correlated with an average CN.[92] Typically, these parameters are obtained by obtaining the linear fit of $(n^2–1)^{-1}$ vs E^2 to find E_0 and E_d, or $(n^2–1)$ vs λ to find E_l after the other parameters are obtained. It has been shown that these parameters can also be predicted *a priori*[91] from the parameters of the constituent oxides and the mole fractions as

$$E_j = \sum_i x_i E_{j,i} \tag{30}$$

where E_j is the j-th energy parameter (i.e., E_0, E_d, and E_l), $E_{j,i}$ are the oxide components (i.e., $E_{0,\mathrm{Bi}}$, $E_{d,\mathrm{Bi}}$, $E_{d,\mathrm{Ga}}$, $E_{l,\mathrm{Pb}}$, etc.), and x_i are the mole fractions of each oxide in the glass. These predicted and measured dispersion parameters, the latter extracted from the indices obtained by prism coupler experiments and modeled with a Sellmeier equation, are shown in Table VIII.

Based on the determined dispersion parameters, the refractive index is back calculated and shown in Table IX. The Wemple–DiDomenico description, with parameters extracted from measured index data $n(\mathrm{WD_{meas}})$, well describes the dispersion for these heavy metal oxide glasses within ±0.3% up to 3.4 μm in the infrared. However, the index values determined from calculated dispersion parameters from oxide components, $n(\mathrm{WD_{calc}})$, underestimate the refractive index by 3%–4% (see Fig. 5). As Fig. 6 shows, optical basicity obtained from the optical gap of oxide components, $n(\Lambda_{E_g})$, as described previously, more closely estimates the visible index than does the index calculated from the dispersion parameters of oxide components, $n(\mathrm{WD_{calc}})$, underestimating the measured values by only about 2%.

IV. Discussion

Calculations of optical basicity have to assume a valence and coordination for the constituent cations. For the calculations here, Pb^{2+}(CN = 4) and Bi^{3+}(CN = 6) were used so that all basicity scales could be compared. EXAFS investigations of Bi_2O_3–PbO–Ga_2O_3 glasses indicate that the oxygen coordination number (CN) of Pb is reduced from CN = 4 in pure PbO to CN = 3.5 in 25 mole% Ga_2O_3 with PbO to only CN = 3 in 40 mole% Bi_2O_3 with PbO.[85] Thus, the formation of PbO_4 tetrahedra is inhibited with decreasing PbO content. The local structure around Bi in these glasses is generally assumed to be BiO_5 and BiO_6 polyhedra as discussed previously. There is some question as to the presence of Bi^{3+} versus Bi^{5+} in HMO glasses. In a recent paper, Fan *et al.*[93] indicated that from the Bi 4*f* peak in the X-ray photoelectron spectroscopy (XPS) spectrum of their Bi_2O_3–B_2O_3–Ga_2O_3 glass system, Bi^{5+} was coexisting

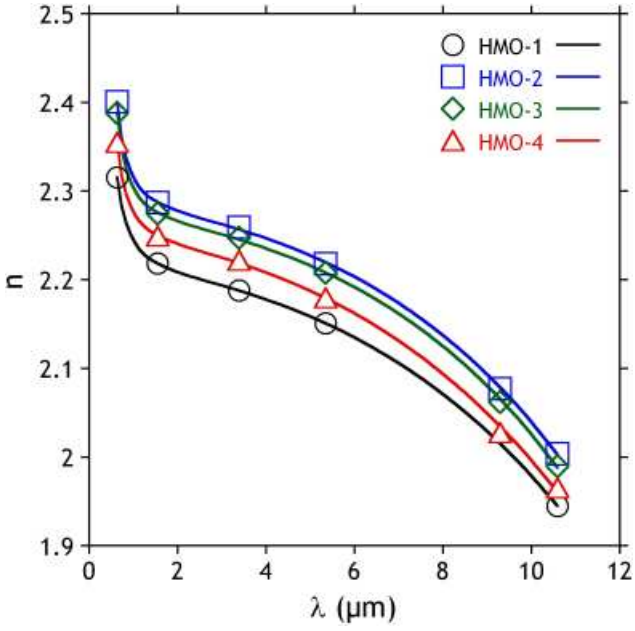

Fig. 2. Measured refractive index (points) and Sellemeir fit (lines). Error bars on the measured refractive index points are smaller than the symbols.

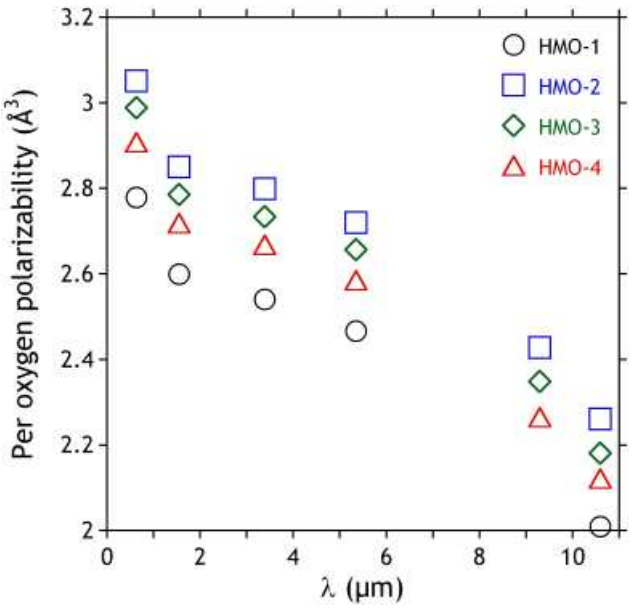

Fig. 3. Calculated per oxygen polarizability dispersion based on the measured refractive index.

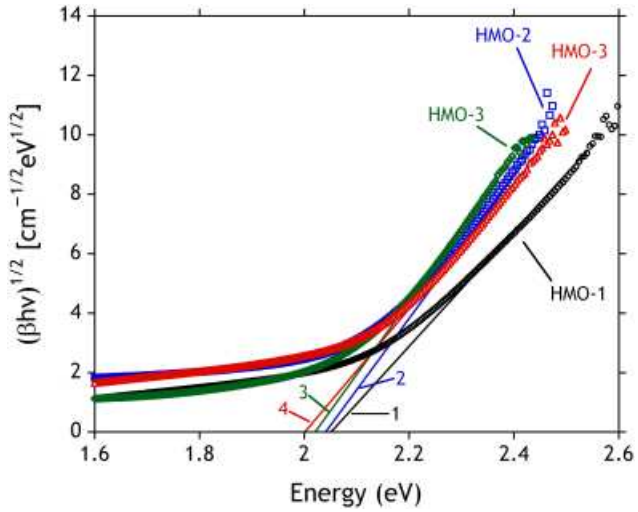

Fig. 4. Optical Gap from the Tauc plot.

with Bi^{3+} in compositions with only 5 mol% Ga_2O_3, but Bi^{5+} decreased in favor of Bi^{3+} with increasing Ga_2O_3 content. On the other hand, Shimizugawa *et al.*[94] from their EXAFS and XPS note that the Bi in their glasses, which are primarily Bi_2O_3–SiO_2–B_2O_3, is almost completely Bi^{5+}. EXAFS data in PbO–Ga_2O_3 glasses indicate that Pb is in the 2+ oxidation state.[95]

Recently, Qi *et al.*[96] showed a remarkable correlation between the per oxygen electronic polarizability and density in binary glass systems containing antimony or bismuth. The correlation was particularly strong with borate and phosphate glasses, with different slopes of density versus oxygen polarizability for different binary systems. The results of this analysis in Fig. 7 show that in the lead–bismuth–gallate glass system, the linear correlation is remarkable ($R^2 = 0.98$) when plotting the oxygen polarizability determined from the optical basicity of oxide energy gaps versus the measured Archimedes density. It can be seen from Table VII that the R_m/V_m values are very similar for these glasses. However, the molar refractivity is based on the total molar polarizability ($\alpha_{m,tot}$) and so includes contributions from both the molar cation polarizability ($\alpha_{m,cat}$) and the molar oxygen polarizability ($\alpha_{m,ox}$). Correlations between these polarizabilities and the density (not shown) were inferior to those using the per oxygen polarizability.

Furthermore, Dimitrov and Komatsu[23] have shown a correlation between the Yamashita–Kurosawa interaction parameter, optical basicity, and oxygen-binding energy. The Yamashita–Kurosawa interaction parameter (A)[97] describes the interaction between cations and anions in terms of the change in the polarizability of the free anion due to the cation as

$$A = \frac{\alpha_f - \alpha_{ox}}{2(\alpha_f - \alpha_{cat})(\alpha_{ox} - \alpha_{cat})} \tag{31}$$

Here, α_f is the electronic polarizability of the free oxide ion, taken to be 3.921 Å^3 (Pauling's value), α_{ox} is the per oxygen polarizability in the oxide as determined by the refractive index and the Lorentz–Lorenz equation, and α_{cat} is the tabulated cation polarizability (assumed to be the same value for free ion and oxide because the electron cloud of the cation is not as deformable as the oxygen ion). This interaction parameter represents the charge overlapping of the anion with its nearest-neighbor cation, and hence is a measure of covalency. Therefore, it is inversely proportional to optical basicity, which is a measure of ionicity.[98] Dimitrov and Komatsu[23] have determined the interaction parameter for various binary oxides and shown that high oxygen polarizability in the oxide is correlated to cations with large ionic radii and large cation polarizability (such as Bi and Pb). The calculation of the interaction parameter (A) of a multioxide system is identical to that for optical basicity as shown in Eq. (30) but substituting the component oxide values of A. The correlation (not shown) between the interaction parameter of the HMO glasses studied here with per oxygen electronic polarizability is excellent ($R^2 = 0.975$) and still very good when correlated with optical basicity from energy gaps ($R^2 = 0.938$). The values for the interaction parameter for component oxide parameters and glasses are shown in Tables III and IV, respectively.

Figure 7 summarizes these observations for the lead–bismuth–gallate glasses studied here. The per oxygen electronic polarizability (α_{ox}) is positively linearly correlated with measured density and with the total cation polarizability ($\alpha_{m,cat}$). The total polarizability, on the other hand, depends on contributions from both the cation and the oxygen atoms from each of the oxides. Thus, even though α_{ox} and $\alpha_{m,cat}$ are almost identical for HMO-2 and HMO-3, their total polarizabilities ($\alpha_{m,tot}$) and hence their refractive indices are quite different because the fractional number of oxygen atoms (F_{ox}) is different. Another way to consider this is to compute the polarizability contributed per mole of a given oxide. Using the per cation polarizability (α_{cat}) and the refractive index or the energy gap, the values of the oxygen polarizability for each oxide ($\alpha_{ox,oxide}$) can be determined.[23] Then the total polarizability contributed by each oxide is just computed as in Eq. (22) with the mole fraction of each oxide applied to compute the total polarizability of the glass this way (see Tables X and XI).

Figure 8 shows the total polarizability in the glass computed in this way, which, although not numerically equal to that determined through optical basicity, is completely correlated ($R^2 = 0.9988$). The index computed with the Lorentz–Lorenz equation using these oxide polarizabilities is also shown in Fig. 6, showing that it overpredicts the measured index at 633 nm by 3%–4%. This method allows inspection of the contribution of substituting oxides on a molar basis. Figure 9 shows that in the glass studied here, Bi_2O_3 contributed to the refractivity/polarizability far more than PbO even though the molar fraction of PbO was higher in HMO-1 and equal to that of Bi_2O_3 in HMO-3 and HMO-4. This is the case because Bi_2O_3, although having a cation that is not as polarizable, contributes two of them in addition to three oxygens with greater polarizability than the oxygen in PbO. This leads to a total polarizability per mole about twice that of PbO. Because Bi_2O_3 is more polarizable than PbO, as also noted by Fujino *et al.*,[65] substituting more Bi_2O_3 for PbO should increase the index, which it does going from HMO-3 to HMO-2. Calculations of this kind based on total oxide polarizability were performed for the approximate glass-forming region of Ga_2O_3–

Table VII. Experimentally Determined Energies and Calculated Refractivity Ratios Using the Optical Basicity Based on the Energy Gap of the Oxides as Input

Glass	α_{m,ox,E_g} (Å^3)	$\alpha_{m,cat}$ (Å^3)	α_{m,tot,E_g} (Å^3)	R_{m,E_g} (cm^3/mol)	V_m, (cm^3/mol)	R_m/V_m	E_g (Eq. (9))	E_g (Eq. (11))	E_{opt} (eV)	ΔE_{Urb} (eV)
HMO-1	5.56	2.70	8.26	20.81	35.70	0.583	3.47	2.23	2.05	0.17
HMO-2	6.73	2.85	9.58	24.13	40.00	0.603	3.15	2.16	2.04	0.13
HMO-3	6.35	2.88	9.23	23.26	38.39	0.606	3.10	2.15	2.02	0.14
HMO-4	6.23	2.73	8.96	22.58	38.16	0.592	3.33	2.20	2.00	0.17

Table VIII. Single Oscillator Dispersion Parameters for the Wemple–DiDomenico Model for the Component Oxides[91] and for Lead–Bismuth–Gallate Glasses (This Work)

	E_0 (eV)		E_d (eV)		E_l (eV)	
Composition/Additive	Exp	Calc	Exp	Calc	Exp	Calc
Ga_2O_3	9.5		16		0.125	
PbO	4.7		23		0.071	
Bi_2O_3	5		21		0.084	
HMO-1	5.73	5.89	22.07	20.80	0.1336	0.0873
HMO-2	5.403	5.56	22.30	20.99	0.1358	0.0853
HMO-3	5.404	5.55	22.03	21.10	0.1353	0.0846
HMO-4	5.54	5.78	22.00	20.80	0.1375	0.0870

$PbO–Bi_2O_3$,[5,65] and the results are shown plotted in the ternary diagram in Fig. 10.

V. Conclusions

Photonics applications often require the creation of materials with given refractivity properties (e.g., density, refractive index). In this paper, we have shown that reasonable estimates of both the refractive index and the density can be derived strictly from the composition. A set of high-density heavy metal oxide glasses based on PbO, Bi_2O_3, and Ga_2O_3 was produced, and their refractive index dispersions, optical energy gaps, and densities were determined experimentally.

The refractive indices and energy gaps were also predicted from the composition using three different approaches for computing the optical basicity and were compared with the measured data. Dispersion parameters for a single oscillator model were determined both from the experimental refractive indices and from calculated dispersions based on molar fractions of the oxide constituents. Assuming only a composition and tabulated values, the prediction of the refractive index in the visible (i.e., at 0.6328 μm) determined from dispersion parameters (i.e., E_0, E_d, E_l) was inferior to the best prediction from optical basicity. For the set of heavy metal oxide glasses studied, the measured refractive index in the visible (0.6328 μm from HeNe) correlated most closely with the predicted index from the optical basicity determined from the energy gap of the oxides PbO, Bi_2O_3, and Ga_2O_3. This worked better than basing the predicted index on optical basicity from EN or ionic–covalent parameter considerations.

Single oscillator dispersion parameters obtained using measured data reproduce the data within ±0.3% out to 3.4 μm in the infrared, but calculated dispersion parameters from oxides underestimate the index by 3%–4%. The predicted glass index from optical basicity, based on component oxide energy gaps, underpredicts the index at 0.633 μm by only 2%, while other basicity scales are less accurate. The predicted energy gap of the glasses based on this optical basicity overpredicts the Tauc

Table IX. Refractive Index Dispersions Measured and Calculated, Rounded to the Nearest 0.001

Glass	Λ (μm)	n_{meas}	n (WD_{meas})	n (WD_{calc})	n (Λ_{E_g})
HMO-1	0.6328	2.315	2.313	2.228	2.281
	1.5473	2.218	2.214	2.142	
	3.39	2.188	2.195	2.127	
HMO-2	0.6328	2.401	2.397	2.303	2.360
	1.5473	2.287	2.280	2.201	
	3.39	2.260	2.257	2.184	
HMO-3	0.6328	2.388	2.385	2.312	2.371
	1.5473	2.275	2.268	2.208	
	3.39	2.248	2.246	2.191	
HMO-4	0.6328	2.355	2.351	2.250	2.315
	1.5473	2.249	2.243	2.159	
	3.39	2.222	2.221	2.143	

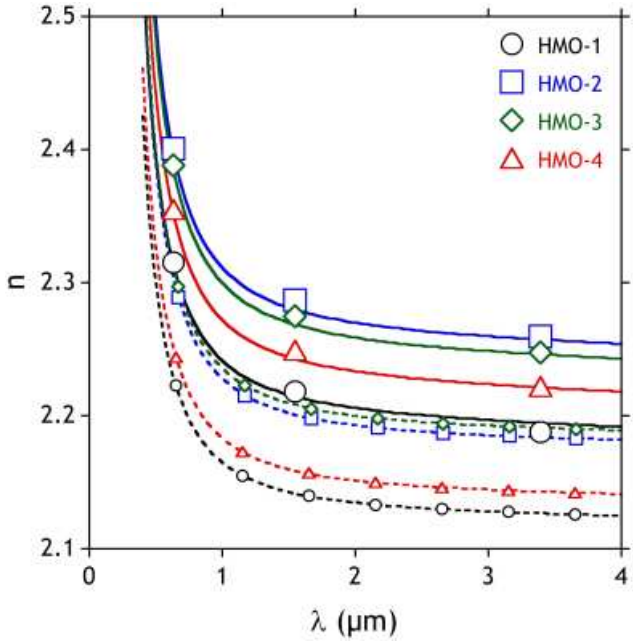

Fig. 5. Wemple–DiDomenico (WD) model for glasses. Large data points show the measured index values (error bars smaller than symbols), and solid lines connecting them show the single oscillator dispersions calculated from the measured index data. Small data points and dotted lines connecting them correspond to the single oscillator model using calculated WD parameters from constituent oxide data.

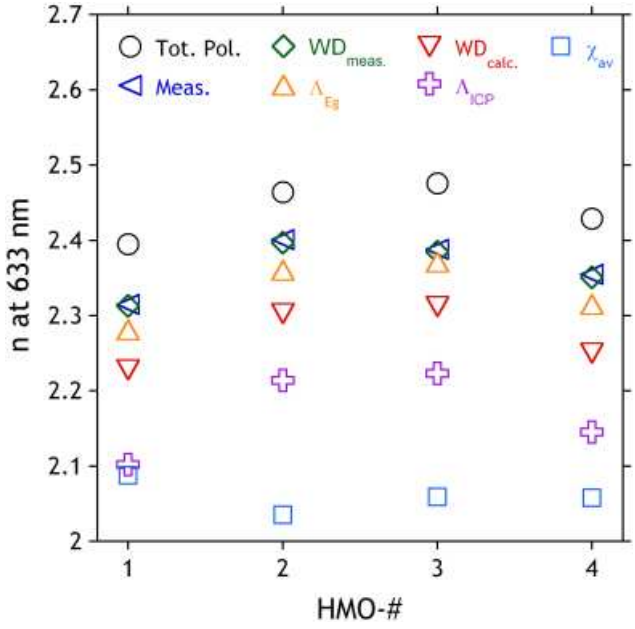

Fig. 6. Calculated versus measured refractive index (633 nm) for four HMO glasses studied. "Tot. pol" refers to the index determined from total oxide polarizability, "Meas." is the measured index using the prism coupler, and "$WD_{meas.}$" refers to the index calculated for Wemple–DiDomenico (WD) single oscillator dispersion parameters derived from the measured data. "Λ_{E_g}" is the index calculated from the optical basicity using oxide energy gaps, and "$WD_{calc.}$" is the index calculated from the WD dispersion obtained from the oxide parameters. "Λ_{ICP}" is the index calculated from optical basicity obtained by the ICP, and "χ_{av}" is the index calculated from the optical basicity determined by the average EN.

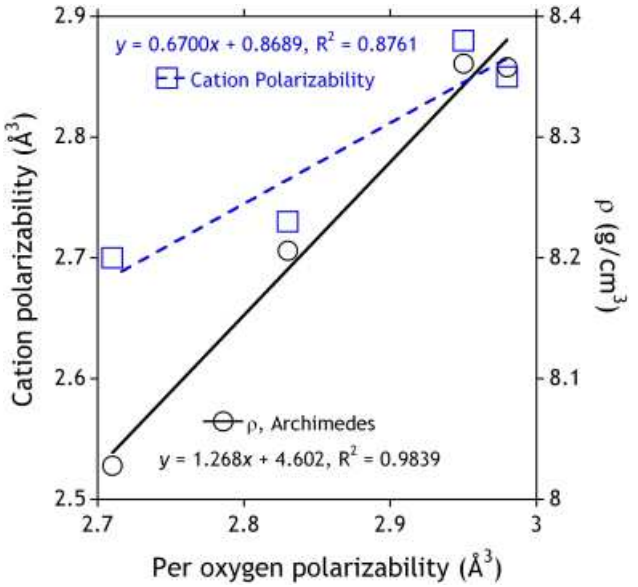

Fig. 7. Measured Archimedes density (Table I) and total cation polarizability (Table IV) as a function of per oxygen polarizability (Table IV) for the glasses studied.

optical gap as determined by transmission measurements by 6%–10%.

These results show that for this system, the density, the refractive index in the visible, and the energy gap can be reasonably predicted using only composition, optical basicity values for the constituent oxides, and partial molar volume coefficients. While basicity predictions provide better accuracy than the oscillator model (given existing literature parameters on heavy metal oxides), they do not provide dispersion information as does the single oscillator model. Calculations such as these are useful for *a priori* prediction of the optical properties of glasses.

Additionally, a method for assessing the effect of various oxides on total polarizability was shown, indicating that both the cation and the oxygen polarizability for each mole of oxide must be considered when designing glass with a particular desired refractivity. Finally, the density must also be considered because it has been shown to correlate with per oxygen polarizability.

This study has shown that predicting the refractive index and the energy gap of glasses is feasible using the concepts of optical basicity. Combined with a prediction of density, this allows a good estimate of the refractivity properties of oxide glasses. However, given the several choices of optical basicity scales and correlation functions, it is not always obvious which tabulated data to use. For the particular set of compositions studied here, a preferred set of input data was selected, the optical basicity that was based on the band gap of the component oxides. Further studies like this one are needed to assess whether this result is particular to this glass family or whether it holds more widely. Although the optical basicity prediction yielded the best estimate of index, the total polarizability method allowed the relative effects of substitutions on the absolute index to be estimated. The oscillator models, while not capable of predicting the absolute index as well as optical basicity does, provides an insight into the effects of individual oxides on the total dispersion. Both absolute index and dispersion are extremely useful optical properties to predict for future photonic applications, and we have shown how this might be accomplished to aid in material design and selection.

Table X. Per Oxide Polarizabilities (in Å^3)

	α_{cat}		$\alpha_{ox,\,oxide}$		$\alpha_{tot,\,oxide}$
	Each cation[23]	All cations	Each oxygen[23]	All oxygens	All ions in oxide
Ga_2O_3	0.195	0.39	1.822	5.47	5.86
PbO	3.623	3.62	3.381	3.38	7.00
Bi_2O_3	1.508	3.02	3.507	10.52	13.54

Table XI. Contributions of Each Oxide to the Total Polarizability of the Glass (All Units in Å^3 Except Refractive Index)

	Ga_2O_3	PbO	Bi_2O_3	$\alpha_{tot,\,oxide}$	$\alpha_{m,\,tot}$ (Λ_{E_g})	$n_{tot,\,oxide}$
HMO-1	1.35	3.33	3.99	8.67	8.26	2.395
HMO-2	0.88	2.59	6.50	9.97	9.58	2.464
HMO-3	0.88	2.98	5.75	9.61	9.23	2.476
HMO-4	1.17	2.80	5.41	9.39	8.96	2.429

Appendix: Equivalency in Various Dispersion Equations

Over the years, authors have used different parameterizations of the single oscillator dispersion description of the refractive index or the dielectric constant.[99] We have presented one approach, the Wemple–DiDomenico, which has been shown to provide information about coordination and dispersion. Other authors have used different versions, including the one-term Sellmeier[100] and the Drude–Voigt equation.[65] The equivalency of these is demonstrated below, and the conversions among them are derived.

First is the original Wemple–DiDomenico (see Eq. (29)), already discussed in the body of this paper, but simplified here to leave off the lattice energy and only focus on the dispersion caused by electronic transitions:

$$n^2 - 1 = \frac{E_0 E_d}{E_0^2 - E^2} \text{ or } \frac{1}{n^2 - 1} = \frac{E_0^2 - E^2}{F} \tag{A-1}$$

Here, F is the oscillator strength in units of eV^2.

Next is the one-term Sellmeier

$$n^2 - 1 = \frac{A_0 \lambda^2}{\lambda^2 - \lambda_0^2} \text{ or } \frac{1}{n^2 - 1} = -\frac{A}{\lambda^2} + B \tag{A-2}$$

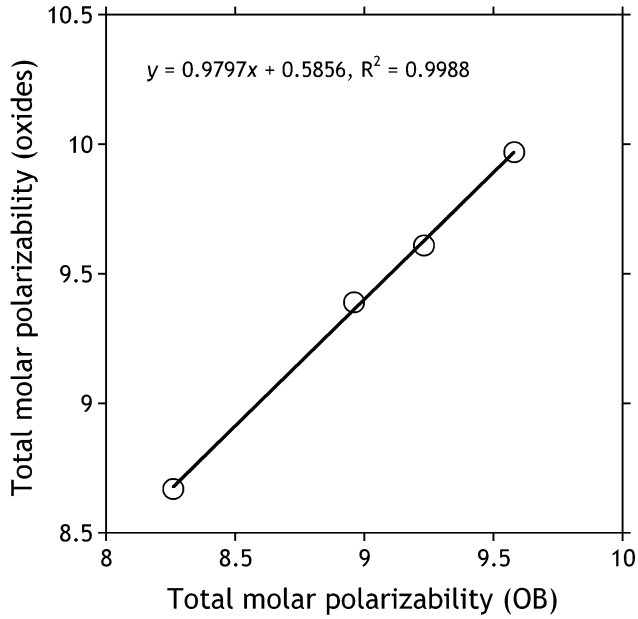

Fig. 8. Correlation between total molar polarizability determined from adding the polarizability of oxides and from adding the optical basicities and converting to polarizability (data from Table XI).

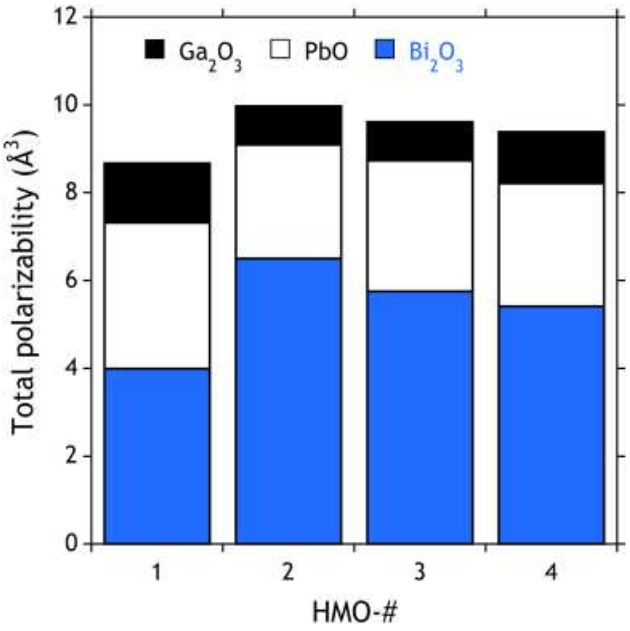

Fig. 9. Relative contributions of constituent oxides to the total polarizability for the glasses studied (data from Table XI).

where $-A$ is the slope and B is the intercept of the linear plot (sometimes indicated as $1/A_0$).

Finally, there is the Drude–Voigt equation

$$n^2 - 1 = \frac{4\pi N e^2}{m_e}\frac{f}{\omega_0^2 - \omega^2} \text{ or}$$
$$\frac{1}{n^2-1} = \frac{\pi m c^2}{e^2 N f}\left(\frac{1}{\lambda_0^2} - \frac{1}{\lambda^2}\right) \quad \text{(A-3)}$$

where f is the unitless oscillator strength, N is the number of oscillators per unit volume ($N = N_{Av}\rho/M$), e is the charge on the electron, m_e is the mass of the electron, ω is the angular frequency, and the product Nf is known as the dispersion.

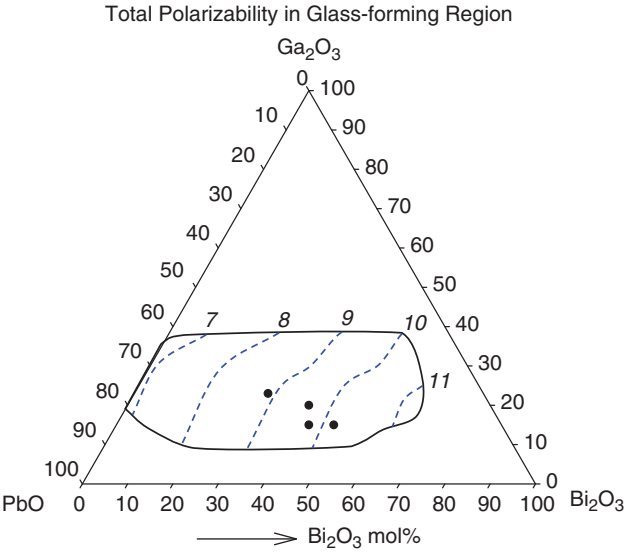

Fig. 10. Total polarizability within the glass-forming region based on oxides for the HMO system studied here. The composition is in mole percent. Data points shown are the glasses made for this study. The calculated total polarizability contours are shown every 1 Å^3. This kind of diagram can be used as a design tool for predicting the refractive index. As explained in the text, the absolute index is slightly overpredicted using this method.

Some parameters that are usually extracted from the latter two dispersions that are not immediately available from the WD equation are (1) n_∞, the refractive index at infinite wavelength considering only electronic transitions, and (2) λ_0, the resonance wavelength of the oscillator driving the index dispersion. The latter is easily obtained directly from the WD parameters[90]:

$$n_\infty = \sqrt{1 + E_d/E_0} = \sqrt{1 + 1/B} \quad \text{(A-4)}$$

The resonance wavelength requires a few more steps. First, the unitless oscillator strength must be calculated as:

$$f(\text{unitless}) = E_d(eV)E_0(eV)\left(\frac{m_e}{4\pi N\hbar^2}\right)$$
$$= \left(1.08 \times 10^7 \frac{\text{cm}^3}{\text{mole}V^2}\right) \quad \text{(A-5)}$$
$$F(eV^2)\left(\frac{M(\text{g/mol})}{\rho(\text{g/cm}^3)}\right)$$

Next, N must be calculated from the density, molar mass, and Avogadro's number, and then the product Nf in m^{-3} can be calculated. Once Nf is determined, the slope parameter A in m^2 from the Sellmeier equation can be determined:

$$A(m^2) = \left(\frac{\pi m_e c^2}{e^2}\right)\left(\frac{1}{Nf}\right)$$
$$= \left(1.01 \times 10^{25}(m^5)\right)\left(\frac{1}{Nf}\right) \quad \text{(A-6)}$$

Now, along with the unitless $A_0 = E_d/E_0$,[100] we can calculate the resonance wavelength.

$$\lambda_0 = \sqrt{A/A_0} = \sqrt{\frac{AE_0}{E_d}} \quad \text{(A-7)}$$

Hence, with these relations, one can perform only one of the dispersion analyses and yet obtain the parameters for several different analyses to compare with the literature.

Given this, we can now show these parameters for our glasses and compare one (HMO-4) with the same composition reported previously as A40.[65] It can be seen that there is good agreement between our HMO-4 and A40, and the differences seen likely lie with the lower measured density for the A40. The glass resonance wavelength can be understood as the average oscillator wavelength of Ga^{3+}, Pb^{2+}, Bi^{3+}, bridging oxygen, and nonbridging oxygen, but is most influenced by the $^1S_0 \rightarrow {}^3P_1$ of Pb^{2+}.[65] The low-energy index, n_∞, calculated here is seen to be too high compared with the measured index at 10.6 μm ($n_{10.6}$) because these oscillator equations do not account for effects of the phonon resonance. Finally, the quantity Nf is correlated with the dispersion or the deviation from flatness of the index versus wavelength curve.

Fujino *et al.*[65] observe that Pb is more dispersive than Bi, and so one would expect the glass with the highest Pb content to be the most dispersive, and in fact, HMO-1 has the highest Pb content (47.5 mol%) and the highest value of Nf, and it shows the smallest value of the dispersion parameter ($\nu_{5.35}$), similar to the Abbe number (V_d), defined as:

$$\nu_{5.35} = \frac{n_{5.35} - 1}{n_{0.633} - n_{10.6}} \text{ and}$$
$$\nu_{d,588\,\text{nm}} = \frac{n_{d,588\,\text{nm}} - 1}{n_{F,486\,\text{nm}} - n_{C,656\,\text{nm}}} \quad \text{(A-8)}$$

	F (eV^2)	f (unitless)	N (m^{-3})	Nf (m^{-3})	ρ (cm^3)	λ_0 (nm)	n_∞	$n_{10.6}$
HMO-1	126.58	4.88×10^{10}	1.69×10^{28}	8.23×10^{38}	8.028	216.9	2.202	1.9447
HMO-2	120.48	5.21×10^{10}	1.51×10^{28}	7.83×10^{38}	8.358	230.2	2.264	2.0035
HMO-3	119.05	4.94×10^{10}	1.57×10^{28}	7.74×10^{38}	8.361	230.2	2.253	1.9897
HMO-4	121.95	5.03×10^{10}	1.58×10^{28}	7.93×10^{38}	8.206	224.4	2.229	1.9652
A40[65]		3.04×10^{10}	2.50×10^{28}	7.61×10^{38}	8.12	228.8		

and

	$\nu_{5.35}$	ν_d
HMO-1	0.427	12.209
HMO-2	0.484	12.271
HMO-3	0.481	19.822
HMO-4	0.460	17.464
A40[65]		

where subscripts are the wavelengths in micrometers when not labeled with units. Larger dispersions are indicated by smaller values of ν. Thus, the dispersion of HMO-1 is the largest when considering the index values through the infrared, that is, including the effects of the phonon dispersion. To calculate the true Abbe number, the Sellmeier formulas derived must be used, and two of the data points are outside the measured range (below 633 nm). If we accept the extrapolation, the Abbe number indicates that when only considering the dispersion caused by electronic transitions (ν_d), HMO-1 still has the highest dispersion as expected.

Acknowledgments

The authors gratefully thank Dong-Sang Kim for helpful discussions and preliminary density models, Norm Anheier for support of the prism coupler, and Joe Ryan and S.K. Sundaram for comments on the manuscript.

References

[1]W. H. Dumbaugh, "Oxide Glasses with Superior Infrared Transmission," *Proc. SPIE*, **505**, 97–101 (1984).
[2]N. F. Borrelli and W. H. Dumbaugh, "Electro- and Magnet-Optic Effects in Heavy Metal Oxide Glasses," *Proc. SPIE*, **843**, 6–9 (1987).
[3]J. Wasylak, E. Golis, and I. Kityk, "Elliptically Induced Second Harmonic Generation in PbO–Bi_2O_3–Ga_2O_3 Glasses," *J. Mater. Sci. Lett.*, **16** [22] 1870–2 (1997).
[4]D. Lorenc, M. Aranyosopva, R. Buczynski, R. Stephien, I. Bugar, A. Vincze, and D. Velic, "Nonlinear Refractive Index of Multicomponent Glasses Designed for Fabrication of Photonic Crystal Fibers," *Appl. Phys. B*, **93**, 531–8 (2009).
[5]W. H. Dumbaugh, J. C. Lapp, and J. E. Shelby, "Heavy Metal Oxide Glasses," *J. Am. Ceram. Soc.*, **75** [9] 2315–26 (1992).
[6]X. Zhao, X. Wang, H. Lin, and Z. Wang, "Correlation Among Electronic Polarizability, Optical Basicity and Interaction Parameter of Bi_2O_3–B_2O_3 Glasses," *Physica B*, **390** [1–2] 293–300 (2007).
[7]J. A. Duffy, "Optical Basicity: A Practical Acid–Base Theory for Oxides and Oxyanions," *J. Chem. Ed.*, **72** [12] 1138–42 (1996).
[8]J. A. Duffy and M. D. Ingram, "Establishment of an Optical Scale for Lewis Basicity in Inorganic Oxyacids, Molten Salts, and Glasses," *J. Am. Chem. Soc.*, **93** [24] 6448–54 (1971).
[9]J. A. Duffy and M. D. Ingram, "An Interpretation of Glass Chemistry in Terms of the Optical Basicity Concept," *J. Non-Cryst. Solids*, **21** [3] 373–410 (1976).
[10]J. A. Duffy, "The Refractivity and Optical Basicity of Glass," *J. Non-Cryst. Solids*, **86**, 149–60 (1986).
[11]V. Dimitrov and T. Komatsu, "Electronic Polarizability, Optical Basicity and Non-Linear Optical Properties of Oxide Glasses," *J. Non-Cryst. Solids*, **249** [2-3] 160–79 (1999).
[12]H. Bach, F. G. K. Baucke, and D. Krause ed. *Electrochemistry of Glasses and Glass Melts, Including Glass Electrodes*. Springer, Berlin, 2001.
[13]F. G. K. Baucke and J. A. Duffy, "The Effect of Basicity on Redox Equilibria in Molten Glasses," *Phys. Chem. Glasses*, **32** [5] 211–8 (1991).
[14]J. A. Duffy, "A Review of Optical Basicity and Its Applications to Oxidic Systems," *Geochim. Cosmochim. Acta*, **57** [16] 3961–70 (1993).
[15]A. Bergman, "Representation of Phosphorus and Vanadium Equilibria Between Liquid Iron and Complex Steelmaking Slags," *Trans. ISIJ*, **28**, 945–51 (1988).
[16]F. Mitchell, D. Sleeman, J. A. Duffy, M. D. Ingram, and R. W. Young, "Optical Basicity of Metallurgical Slags: New Computer Based System for Data Visualization and Analysis," *Ironmaking Steelmaking*, **24** [4] 306–20 (1997).
[17]K. C. Mills, "The Influence of Structure on the Physico-Chemical Properties of Slags," *ISIJ Intern.*, **33** [1] 148–55 (1993).
[18]J. A. Duffy and B. Harris, "Reaction Sites in Network Oxyanion Systems," *Ironmaking Steelmaking*, **22** [2] 132–6 (1995).
[19]P. Moriceau, B. Taouk, E. Bordes, and P. Courtine, "Correlations Between the Optical Basicity of Catalysts and Their Selectivity in Oxidation of Alcohols, Ammoxidation and Combustion of Hydrocarbons," *Catal. Today*, **61** [1–4] 197–201 (2000).
[20]J. A. Duffy, "Chemical Bonding in the Oxides of the Elements: A New Appraisal," *J. Solid State Chem.*, **62** [2] 145–57 (1986).
[21]R. R. Reddy, Y. Nazeer Ahammed, P. Abdul Azeem, K. Rama Gopal, and T. V. R. Rao, "Electronic Polarizability and Optical Basicity Properties of Oxide Glasses Through Average Electronegativity," *J. Non-Cryst. Solids*, **286** [3] 169–80 (2001).
[22]M. Lenglet, "Ligand Field Spectroscopy and Chemical Bonding in Cr^{3+}-, Fe^{3+}-, Co^{2+}- and Ni^{2+}-Containing Oxidic Solids: Influence of the Inductive Effect of the Competing Bonds and Magnetic Interactions on the Degree of Covalency of the 3d M-O Bonds," *Mater. Res. Bull.*, **35** [4] 531–43 (2000).
[23]V. Dimitrov and T. Komatsu, "Effect of Interionic Interaction on the Electronic Polarizability, Optical Basicity and Binding Energy of Simple Oxides," *J. Ceram. Soc. Jpn.*, **107** [11] 1012–8 (1999).
[24]C. K. Jørgenson, *Oxidation Numbers and Oxidation States*. Springer, Berlin, 1969.
[25]Verein-Deutscher-Eisenhuttenleute. ed. *Slag Atlas*, 2nd edition, Verlag Stahleisen GmbH, 1995.
[26]N. Iwamoto, Y. Makino, and S. Kasahara, "Correlation between Refraction Basicity and Theoretical Optical Basicity Part I. Alkaline and Alkaline-Earth Silicate Glasses," *J. Non-Cryst. Solids*, **68** [2–3] 379–88 (1984).
[27]J. A. Duffy, "Use of Refractivity Data for Obtaining Optical Basicities of Transition Metal Oxides," *Ironmaking Steelmaking*, **16** [6] 426–8 (1989).
[28]I. Fanderlik, *Optical Properties of Glass*, Vol. 5. Elsevier, Amsterdam, 1983.
[29]J. R. Tessman, A. H. Kahn, and W. Shockley, "Electronic Polarizabilities of Ions in Crystals," *Phys. Rev.*, **92** [4] 890–5 (1953).
[30]E. Kordes, "Die Ermittlung von Atomabstanden aus der Lichtbrechung," *Z. Phys. Chem. Abt. B*, **44**, 249–60 (1939).
[31]K. Fajans and G. Joos, "Molrefraktion von Ionen und Molekulen im Lichte der Atomstruktur," *Z. Physik*, **23**, 1–46 (1924).
[32]H. W. Jaffe, *Crystal Chemistry and Refractivity*. Cambridge University Press, Cambridge, 1988.
[33]D. Pohl, "Electronic Polarizabilities of Ions in Doubly Refracting Crystals," *Acta Crystallogr. A*, **34**, 574–8 (1978).
[34]J. A. Duffy, "Electronic Polarisability and Related Properties of the Oxide Ion," *Phys. Chem. Glasses*, **30** [1] 1–4 (1989).
[35]J. A. Duffy, "The Electronic Polarisability of Oxygen in Glass and the Effect of Composition," *J. Non-Cryst. Solids*, **297** [2–3] 275–84 (2002).
[36]N. Iwamoto and Y. Makino, "Determination of Ionic Distributions of Three Sorts of Oxygens in a Few Binary Silicate Glasses from Molar Refractivity," *J. Non-Cryst. Solids*, **34** [3] 381–91 (1979).
[37]J. A. Duffy, "Optical Basicity of Aluminosilicate Glasses," *Phys. Chem. Glasses*, **44** [6] 388–92 (2003).
[38]J. A. Duffy, "Relationship between Cationic Charge, Coordination Number, and Polarizability in Oxidic Materials," *J. Phys. Chem. B*, **108** [37] 14137–41 (2004).
[39]J. A. Duffy, "Abnormal Refractivity Trends in Phosphate Glass Systems," *Phys. Chem. Glasses*, **45** [6] 322–7 (2004).
[40]V. Dimitrov and S. Sakka, "Electronic Polarizability and Optical Basicity of Simple Oxides. I," *J. Appl. Phys.*, **79** [3] 1736–40 (1996).
[41]T. Banu, K. K. Rao, and M. Vithal, "Optical, Thermal and Electrical Studies of Nasicon Type $Na_2PbZnMP_3O_{12}$ (M = Al, Fe and Ga) Glasses," *Phys. Chem. Glasses*, **44** [1] 30–5 (2003).
[42]M. Vithal, P. Nachimuthu, T. Banu, and R. Jagannathan, "Optical and Electrical Properties of PbO–TiO_2, PbO–TeO_2, and PbO–CdO Glass Systems," *J. Appl. Phys.*, **81** [12] 7922–6 (1997).
[43]L. Pauling, "The Nature of the Chemical Bond IV. The Energy of Single Bonds and the Relative Electronegativity of Atoms," *J. Am. Chem. Soc.*, **54**, 3570–82 (1932).

[44]J. A. Duffy and M. D. Ingram, "Comments on the Application of Optical Basicity to Glass," *J. Non-Cryst. Solids*, **144**, 76–80 (1992).
[45]J. A. Duffy and M. D. Ingram, "Optical Basicity"; pp. 159–84, in *Optical Properties of Glass*, Edited by D. R. Ulhmann, and N. J. Kreidl. American Ceramic Society, Westerville, OH, 1991.
[46]J. H. Binks and J. A. Duffy, "Ionicity of Simple Binary Oxides," *J. Chem. Soc., Faraday Trans.*, **2** [81] 473–8 (1985).
[47]K. Li and D. Xue, "Estimation of Electronegativity Values of Elements in Different Valence States," *J. Phys. Chem. A*, **110** [39] 11332–7 (2006).
[48]J. Portier, G. Campet, J. Etourneau, and B. Tanguy, "A Simple Model for the Estimation of Electronegativities of Cations in Different Electronic States and Coordinations," *J. Alloys Compd.*, **209** [1–2] 285–9 (1994).
[49]J. Mullay, "Estimation of Atomic and Group Electronegativities," *Struct. Bond.*, **66**, 1–25 (1987).
[50]R. Asokamani and R. Manjula, "Correlation between Electronegativity and Superconductivity," *Phys. Rev. B*, **39** [7] 4217–21 (1989).
[51]R. R. Reddy, Y. Nazeer Ahammed, K. Rama Gopal, P. Abdul Azeem, and T. V. R. Rao, "Correlation between Optical Basicity, Electronegativity and Electronic Polarizability for Some Oxides and Oxysalts," *Opt. Mater.*, **12** [4] 425–8 (1999).
[52]X. Zhao, X. Wang, H. Lin, and Z. Wang, "Average Electronegativity, Electronic Polarizability and Optical Basicity of Lanthanide Oxides for Different Coordination Numbers," *Physica B*, **403** [10–11] 1787–92 (2008).
[53]Y. Zhang, "Electronegativities of Elements in Valence States and Their Applications. 1. Electronegativities of Elements in Valence States," *Inorg. Chem.*, **21** [11] 3886–9 (1982).
[54]J. Portier, G. Campet, J. Etourneau, M. C. R. Shastry, and B. Tanguy, "A Simple Approach to Materials Design: Role Played by an Ionic-Covalent Parameter Based on Polarizing Power and Electronegativity," *J. Alloys Compd.*, **209** [1–2] 59–64 (1994).
[55]Y. Zhang, "Electronegativities of Elements in Valence States and Their Applications. 2. A Scale for Strengths of Lewis Acids," *Inorg. Chem.*, **21** [11] 3889–93 (1982).
[56]R. D. Shannon, "Revised Effective Ionic Radii and Systematic Studies of Interatomic Distances in Halides and Chalcogenides," *Acta Crystallog. A*, **32**, 751–67 (1976).
[57]A. Lebouteiller and P. Courtine, "Improvement of a Bulk Optical Basicity Table for Oxidic Systems," *J. Solid State Chem.*, **137** [1] 94–103 (1998).
[58]ITC Inc., *SciGlass 7.0 Database and Information System*. Build 7.10.05.098, ITC Inc., Hamilton, OH, 2007.
[59]B. G. Aitken and N. F. Borrelli, *Thallium Gallate Glasses*, USPTO, 5168079, Corning Inc., Corning, NY, 1992.
[60]Y. G. Choi and J. Heo, "Influence of OH^- and Nd^{3+} Concentrations on the Lifetimes of the Nd^{3+}: $^4F_{3/2}$ Level in PbO–Bi_2O_3–Ga_2O_3 Glasses," *Phys. Chem. Glasses*, **39** [6] 311–7 (1998).
[61]W. H. Dumbaugh, "Heavy Metal Oxide Glasses Containing Bi_2O_3," *Phys. Chem. Glasses*, **27** [3] 119–23 (1986).
[62]O. H. El-Bayoumi, A. A. Said, R. J. Andrews, M. J. Suscavage, T. P. Swiler, J. H. Simmons, and E. W. Van Srtyland, "High Refractive Index Glasses"; 91-96 in Proc. Boll.Soc.Espan.Ceram.Vidrio. 31-C (3). Proc. XVI Intern.Congr.on Glass, (1992).
[63]J. Filipecki, E. Golis, I. V. Kityk, J. Wasylak, and M. Janewicz, "Glassy State and Structural Analysis of Lead-Bismuth Oxide Glasses"; 297-302 in 2. Proc.X-VIIth Intern.Congr.on Glass, (1995).
[64]S. Fujino, H. Takebe, and K. Morinaga, "Measurements of Refractive Indexes and Factors Affecting Dispersion in Oxide Glasses," *J. Am. Cer. Soc.*, **78** [5] 1179–84 (1995).
[65]S. Fujino, H. Takebe, and K. Morinaga, "Effect of PbO, Bi_2O_3 and Tl_2O on Optical Properties of Heavy-Metal Gallate Glasses," *J. Ceram. Soc. Jpn.*, **103** [4] 340–5 (1995).
[66]D. W. Hall, M. A. Newhouse, N. F. Borrelli, W. H. Dumbaugh, and D. L. Weidman, "Nonlinear optical Susceptibilities of High-Index Glasses," *Appl. Phys. Lett.*, **54** [14] 1293–5 (1989).
[67]J. Heo, C. G. Kim, and Y. S. Kim, "Characterization and X-Ray Photoelectron Spectroscopy Investigation of PbO–Bi_2O_3–Ga_2O_3 Glasses," *J. Am. Ceram. Soc.*, **78** [5] 1285–0 (1995).
[68]S. Inaba, S. Oda, and K. Morinaga, "Equation for Estimating the Thermal Diffusivity, Specific Heat and Thermal Conductivity of Oxide Glasses," *J. Jpn. Inst. Metals*, **65** [8] 680–7 (2001).
[69]S. Inaba, S. Oda, and K. Morinaga, "Heat Capacity of Oxide Glasses at High Temperature Region," *J. Non-Cryst. Solids*, **325** [1–3] 258–66 (2003).
[70]M. Janewicz, J. Wasylak, E. Czerwosz, and R. Diduszko, "Structure and Properties of Ga_2O_3–PbO–Bi_2O_3 Glasses"; pp. 265–270, in *Proc. Boll. Soc. Espan. Ceram. Vidrio*, 31-C (3), Proc. XVI Intern. Congr. on Glass, 1992.
[71]C. G. Kim, J. Heo, and Y. S. Kim, "Preparation and Characteristics of Infrared Transmitting Glasses in the PbO–Bi_2O_3–Ga_2O_3 System," *J. Kor. Ceram. Soc.*, **30** [9] 709–16 (1993).
[72]J. C. Lapp, "Alkali Bismuth Gallate Glasses," *Am. Ceram. Soc. Bull.*, **71** [10] 1453–549 (1992).
[73]J. C. Lapp, W. H. Dumbaugh, and M. L. Powley, "Heavy Metal Oxide Glass," *Riv. Staz. Sper. Vetro*, **19** [1] 91–6 (1989).
[74]J. C. Lapp, W. H. Dumbaugh, and M. L. Powley, "Recent Advances in Heavy Metal Oxide Glass Research," *Proc. SPIE*, **1327**, 162–70 (1990).
[75]H. Wenhai, C. S. Ray, and D. E. Day, "Heavy Metal Oxide Glass. Part I. Preparation and Properties," *Glass and Enamel*, **21** [4] 1–8 (1993).
[76]H. Wenhai, C. S. Ray, and D. E. Day, "Heavy Metal Oxide Glass. Part II. Structure Aspect and Crystallization Behavior," *Glass and Enamel*, **21** [6] 1–12 (1993).
[77]H. Wenhai, C. S. Ray, and D. E. Day, "Color and Selected Properties of PbO–$BiO_{1.5}$–$GaO_{1.5}$ Glasses," *J. Am. Ceram. Soc.*, **77** [4] 1017–24 (1994).
[78]H. Wenhai, C. S. Ray, and D. E. Day, "Formation and Properties of PbO–$NbO_{2.5}$–TeO_2 Glasses"; pp. 395–401 in 5. *Proceedings of XVIIth International Congress on Glass*, Beijing 1995.
[79]J. A. Ruller and J. E. Shelby, "Properties of Heavy Metal Oxide Glasses," *Phys. Chem. Glasses*, **33** [5] 177–83 (1992).
[80]L. C. Courrol, L. R. P. Kassab, M. E. Fukumoto, N. U. Wetter, S. H. Tatumi, and N. I. Morimoto, "Spectroscopic Properties of Heavy Metal Oxide Glasses Doped with Erbium," *J. Lumin.*, **102 and 103**, 91–5 (2003).
[81]J. A. Duffy, "Optical Basicity Analysis of Glasses Containing Trivalent Scandium, Yttrium, Gallium and Indium," *Phys. Chem. Glasses*, **46** [5] 500–4 (2005).
[82]N. Iwamoto, Y. Makino, and S. Kasahara, "Correlation between Refraction Basicity and Theoretical Optical Basicity Part II. PbO–SiO_2, CaO–Al_2O_3–SiO_2 and K_2O–TiO_2–SiO_2 Glasses," *J. Non-Cryst. Solids*, **68** [2–3] 389–97 (1984).
[83]J. A. Duffy, "The Optical Basicity and UV Absorption Spectra of Lead Metasilicate and Lead Monoxide," *J. Non-Cryst. Solids*, **76** [2–3] 391–7 (1985).
[84]F. Miyaji, K. Tadanaga, T. Yoko, and S. Sakka, "Coordination of Ga^{3+} Ions in PbO–Ga_2O_3 Glasses as Determined by ^{71}Ga NMR," *J. Non-Cryst. Solids*, **139**, 268–70 (1992).
[85]Y. G. Choi, K. H. Kim, V. A. Chernov, and J. Heo, "EXAFS Spectroscopic Study of PbO–Bi_2O_3–Ga_2O_3 Glasses," *J. Non-Cryst. Solids*, **259** [1–3] 205–11 (1999).
[86]J. Tauc ed. *Amorphous and Liquid Semiconductors*. Plenum Press, London, 1974.
[87]S. Kasap, and P. Capper ed. *Springer Handbook of Electronic and Photonic Materials*. Springer, Berlin, 2006.
[88]M. Kranjcec, I. P. Studenyak, and M. V. Kurik, "On the Urbach Rule in Non-Crystalline Solids," *J. Non-Cryst. Solids*, **355** [1] 54–7 (2009).
[89]A. K. Sandhu, S. Singh, and O. P. Pandey, "Neutron Irradiation Effects on Optical and Structural Properties of Silicate Glasses," *Mater. Chem. Phys.*, **115** [2–3] 783–8 (2009).
[90]S. H. Wemple and M. DiDomenico, "Behavior of the Electronic Dielectric Constant in Covalent and Ionic Materials," *Phys. Rev. B*, **3** [4] 1338–51 (1971).
[91]R. N. Brown, "Material Dispersion in Heavy Metal Oxide Glasses Containing Bi_2O_3," *J. Non-Cryst. Solids*, **92**, 89–94 (1987).
[92]S. H. Wemple, "Refractive-Index Behavior of Amorphous Semiconductors and Glasses," *Phys. Rev. B*, **7** [8] 3767–77 (1973).
[93]H. Fan, G. Wang, and L. Hu, "Infrared, Raman and XPS Spectroscopic Studies of Bi_2O_3–B_2O_3–Ga_2O_3 Glasses;" *Solid State Sci.*, **11** [12] 2065–70 (2009).
[94]Y. Shimizugawa, N. Sugimoto, and K. Hirao, "X-Ray Absorption Fine Structure Glasses Containing Bi_2O_3 with Third-Order Non-Linearities," **221** [2–3] 208–12 (1997).
[95]Y. G. Choi, K. H. Kim, V. A. Chernov, and J. Heo, "Pb LIII-Edge EXAFS and XANES Analyses on the Structural Environment of Lead in PbO–Ga_2O_3 Glasses," *J. Non-Cryst. Solids*, **246** [1–2] 128–35 (1999).
[96]J. Qi, D. Xue, H. Ratajczak, and G. Ning, "Electronic Polarizability of the Oxide Ion and Density of Binary Silicate, Borate and Phosphate Oxide Glasses," *Physica B*, **349** [1–4] 265–9 (2004).
[97]J. Yamashita and T. Kurosawa, "The Theory of the Dielectric Constant of Ionic Crystals III," *J. Phys. Soc. Jpn.*, **10** [8] 610–33 (1955).
[98]V. Dimitrov and T. Komatsu, "Interionic Interactions, Electronic Polarizability and Optical Basicity of Oxide Glasses," *J. Ceram. Soc. Jpn.*, **108** [4] 330–8 (2000).
[99]A. M. Efimov, *Optical Constants of Inorganic Glasses*. CRC Press, Boca Raton, FL, 1995.
[100]R. D. Shannon, R. C. Shannon, O. Medenbach, and R. X. Fischer, "Refractive Index and Dispersion of Fluorides and Oxides," *J. Phys. Chem. Ref. Data*, **31** [4] 931–70 (2002). □